ICAST2014 #094

Air-coupled ultrasound for damage detection in CFRP using Lamb waves and ultrasonic verification

G. Alleman[1,2], M.M.J.M. Pelt[2], R.M. Groves[1]*

[1] Aerospace Non-Destructive Testing Laboratory, Delft University of Technology, Delft, The Netherlands
[2] Aviation Department, University of Applied Sciences, Amsterdam, The Netherlands

Abstract

Modern aircraft consist of Carbon Fiber Reinforced Polymer (CFRP) structures and require advanced non-destructive testing (NDT) techniques to detect barely visible impact damage (BVID). Conventional NDT methods, based on manual, or automated, scanning with ultrasonic transducers with water or gel couplant are time consuming for larger areas. Ultrasonic Lamb waves are of interest for structural health monitoring (SHM) of aircraft and have been investigated previously for this application by the authors and others. Lamb waves are guided by the plate-like aircraft structure and for SHM applications an array of permanently fixed embedded or surface-mounted piezoelectric transducers (PZTs) can be used to monitor large surface areas by using Lamb waves.

This paper describes the novel combination of air-coupled ultrasound transducers (ACTs) and Lamb wave sensing using ultrasonic verification (USV). USV is an analysis procedure of monitoring the structural health of CFRP, developed jointly by the University of Amsterdam and the University of Applied Sciences, Amsterdam. For the scanning of larger structures, fixed transducers are not desirable to avoid damage to the surface by contact between the probe head and the couplant. ACTs can overcome these problems by using air as a couplant. Developments in ACT technology now allow much higher energy transfer between the transducer and the structure, making the technology more accessible for aerospace applications. The objectives of this research were to determine the optimum transducer parameters for damage detection in CFRP and to determine if ACTs can be used as alternative for PZTs when applying the USV procedure. A Design Of Experiments (DOE) with the variables frequency, type of transducer, distance between the transducer and the material, wave mode and angle of incidence determined the parameters with the highest sensitivity to detect damage. A damage test comparing the fidelity and pulse energy methods showed that damage can be detected best with the energy method based on the variances between the measurements, difference in percentage between undamaged and damaged signals and time windows in which damage can be detected. Because damage can be detected in CFRP, ACTs can be used as alternative for PZTs in USV.

* Dr Roger Groves, r.m.groves@tudelft.nl

1. INTRODUCTION

Modern aircraft such as the Boeing 787 and the Airbus A350, which consist of a high percentage Carbon Fiber Reinforced Polymer (CFRP) structures, require advanced Non Destructive Tests (NDTs) to detect damages and imperfections which are difficult to detect with conventional NDT techniques or are time-consuming. Due to the laminate structure of CFRP, damage inside the material may not be visible with inspection of external surfaces. These damages decrease the mechanical strength and reduce the fatigue life of CFRP [1]. Conventional inspection methods are time consuming and limited in their ability to cover larger areas. In the Ultrasonic Verification (USV) method of monitoring the structural health of CFRP by using ultrasound, a small number of surface mounted piezoelectric transducers (PZTs) are used to monitor large surface areas by comparing the undamaged echo with the real time echo using fidelity [2].

In some cases, fixed transducers are not desirable because fast scanning of an unknown surface is required or because the material may not be touched by the transducers. Air-coupled transducers (ACTs) can overcome these problems by using air instead of a bonded sensor. For ACTs to be used as an alternative for PZTs, the best setting for damage detection must be selected for each situation. The objective of this research is to determine the best setting for ACT to detect damages in flat CFRP and to determine if ACTs can be used as alternative for PZTs in USV.

2. LAMB WAVE THEORY

When an ultrasonic pulse is send into a plate like material, energy can be coupled into Lamb waves. Due to their sensitivity to many failure modes in composite plates, Lamb waves are a valuable tool for damage detection [3, 4]. Ultrasonic transducers couple energy into a structure and excite ultrasonic modes. For plate like structures energy is preferentially coupled into symmetric and asymmetric Lamb wave modes (fig. 1) [5]. Symmetric and asymmetric modes differ in velocity and incidence angle due to wave propagation parameters and are further modified by a difference in material stiffness and density. When damage is located in the material, reflections, scattering and mode conversion take place, which results in modified detected signals. By comparing the undamaged signal with the damaged signal using fidelity and energy described later, damage can be detected.

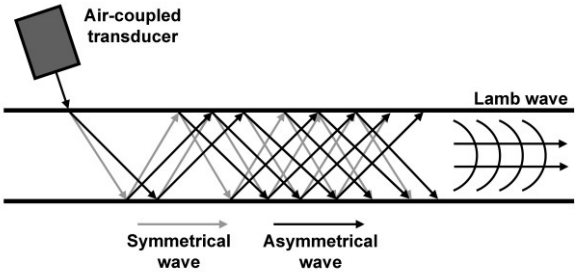

Figure 1. Lamb wave modes

An infinite number of symmetric and asymmetric modes, which differ in velocity, exist for a specific thickness, visualized in dispersion curves [6]. Dispersion curves can be calculated in Matlab™ by solving eq.1 [7] (fig. 2 and fig.3).

$$\frac{\tan(qh)}{\tan(ph)} = \frac{4k^2qp\mu}{(\lambda k^2 + \lambda p^2 + 2\mu p^2)(k^2 - q^2)} \tag{1}$$

Where λ, μ are Lamé constants, k is the wave number, h the thickness, and the parameters p, q are defined as

$$p^2 = \frac{\omega^2}{c_L^2 - k^2}, \quad q^2 = \frac{\omega^2}{c_T^2 - k^2} \tag{2}$$

with ω, c_L and c_T being the angular frequency and the longitudinal and transverse velocities, respectively. At lower frequencies or for thinner materials, fewer modes exist, which makes the analysis less complicated. Therefore, only frequencies where the first symmetric (S_0) and asymmetric (A_0) mode are excited are used in this research.

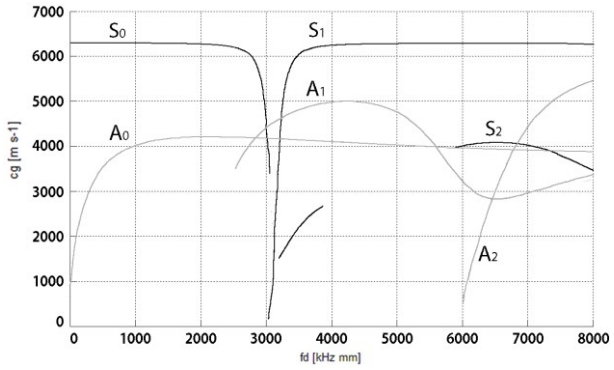

Figure 2. Dispersion curves group velocity

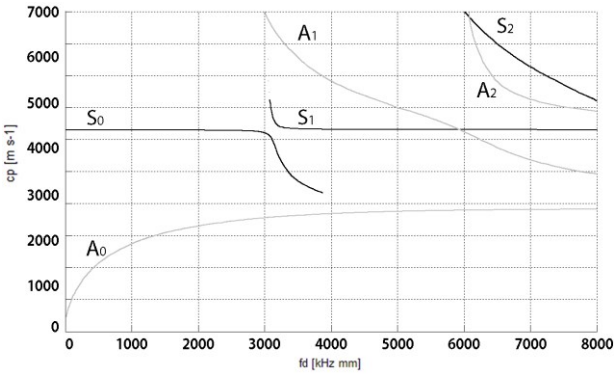

Figure 3. Dispersion curves phase velocity

When a Lamb wave passes from one material to another, mode conversion, scattering, reflection and refraction takes place. The angle of reflection is equal to the angle of incidence, but the angle of refraction depends on the phase velocities of the wave in both materials. The relationship between the phase velocities and angles of refraction of both materials is described in Snell's law (eq. 3) [8].

$$\frac{\sin\theta_1}{V_{L_1}} = \frac{\sin\theta_2}{V_{L_2}} \tag{3}$$

This equation is in terms of sound velocity in air V_{L_1}, phase velocity in CFRP V_{L_2}, the angle of incidence of the transducer θ_1 and the angle of the wave inside the CFRP θ_2. The angle of incidence that makes an angle of refraction of 90° is known as the critical angle. At the critical angle, the waveform travels along the surface of the plate and decays exponentially [8]. If the angle of incidence can be set inside the critical angle, the wave will travel inside the CFRP with the minimum number of reflections.

When sound travels through solid materials, wave propagation occurs due to the elastic bond between molecules or atoms. The ratio between the transverse component of the wave to the speed of the wave is the impedance (eq. 4) [9]. Because ultrasonic waves reflect at the boundaries of the material, a difference in impedance occurs between each side of the boundary, which is called impedance mismatch. A larger impedance mismatch will result in more reflected energy at the boundary.

$$Z = \rho \cdot V \tag{4}$$

This equation is in terms of impedance Z, density ρ and velocity V. With ACTs, air is used as coupling medium between the transducer and the material to transfer the ultrasonic waves. But the main problem with ACTs is the large impedance mismatch that exists between the transducer and air, and between air and the material, which results in a large percentage of energy that will be reflected at the boundaries [10]. The impedance mismatch between the transducer and air has been decreased by later generation of ACTs.

In front of the transducer, the ultrasonic beam can be divided into near field and far field regions (fig. 4). In the near field, the amplitude of the echo will fluctuate and in the far field the amplitude drops to zero [11]. Due to the variations of amplitude within the near field it can be difficult to detect small damages in this field [11]. The near field distance N is calculated with equation 5 in terms of element diameter D, frequency f and material sound velocity c.

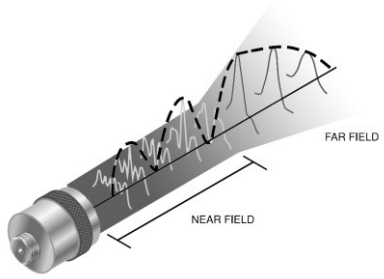

Figure 4. Near field and far field regions.
Reprinted from Olympus NDT, 2006. Retrieved March 3, 2014.

$$N = \frac{D^2 * f}{4 \cdot c} \tag{5}$$

To compare the undamaged signal with the damaged signal, two different methods are used. With the USV method, two signals are compared with fidelity, in which cross-correlation is divided by auto-correlation (eq. 6). This results in a number between 0 and 1 and is therefore dimensionless. The second method to compare signals is based on the difference in energy of the signal. Energy is calculated with equation 7.

$$Fidelity\ (\eta) = \frac{\int_{t1}^{t2} V_1(t) \cdot V_2(t+\tau) \cdot dt}{\sqrt{\left[\int_{t1}^{t2} V_1(t) \cdot V_1(t+\tau) \cdot dt\right] \cdot \left[\int_{t1}^{t2} V_2(t) \cdot V_2(t+\tau) \cdot dt\right]}} \tag{6}$$

$$E = U^2 \cdot R \cdot t \tag{7}$$

Where E is the energy, U is the voltage, R is the resistance of the signal generator (50Ω, frequency dependence unknown) and t is the time.

3. DESIGN OF EXPERIMENT

To provide a better understanding of ACTs, an exploratory study was performed to select the cause-and-effect relationship between variables. This experiment was a factorial experiment approach, testing all possible combinations of variables, because all variables are related to each other.

For this research, three different ACTs are available, which differ in frequency (350 kHz and 1 MHz) and focus (point focus and plane wave) (table 1). The amount of beam convergence of point focus transducers is indicated by the focal length. Plane wave transducers are not converging and do not have a focal length.

Table 1 Mechanical Properties

Type	Focus	Frequency [kHz]	Focal length [mm]
NCG350-D13-P38	Point focus	350	38
NCG350-D13	Plane wave	350	-
NCT1-D3	Plane wave	1000	-

To indicate the cause-and-effect relationship between the variables frequency, type of transducer, distance between transducer and the plate, wave mode and angle of incidence, a DOE is performed (fig. 5). The distance between the transducer and the plate can be set to in the near field, between the near field distance and the focal length and more than the focal length. The wave modes selected are the first symmetrical (S_0) and asymmetrical (A_0) mode. The distance between the ACT and the PZT is fixed to 50 mm for the DOE [12, 13].

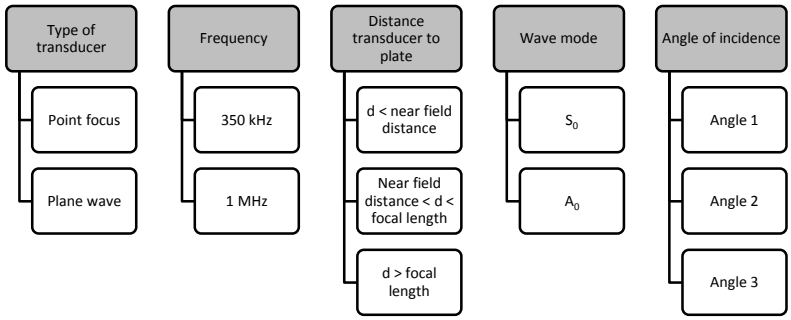

Figure 5. Design of experiments

First, and angle of incidence test was performed to determine the three angles which give the highest energy at the signal output. With these three angles for every transducer and for two wave modes, and the other variables, 42 different combinations were tested. With these settings, a damage detection test was performed to determine if damage can be detected by using ACT. After that, a test with an increasing distance between both transducers was made to indicate the energy loss over the propagation distance.

The USV method is based on fidelity, which divides cross-correlation by auto-correlation and gives a number between 0 and 1 whereby 1 means that both signals are completely identical and 0 indicates no overlap between both signals. But since fidelity is not dependent on the amplitude of the signal and there are always two signals needed to compare, the energy of the signal is used to compare the 42 different

combinations of the DOE. After the optimum setting was selected, fidelity and energy were used to determine if ACTs can be used for damage detection.

A high frequency Gaussian pulse with the specifications described in table 2 is generated by a signal generator (Agilent 33522B) and amplified by a power amplifier (Agilent 33502A) (fig. 6). The sample frequencies are adjusted to the peak frequencies of the calibration form. This signal is sent into a CFRP thermoset plate of 350 mm x 150 mm x 3 mm with a density of 1529 kg/m^3, a Young's modulus of 60.43 GPa and an average Poisson ratio of -0.0539 via one ACT. The ACT is connected to an external inline matching network, which is used to electrically match the transducers to the receiving electronics. With a fixed PZT (Mistras WSα), the signal is received and sent to an oscilloscope (PicoScope 6402A) via another amplifier (Mistras amplifier 20/40/60 dB). In this research, only one ACT is used at a time.

The carbon plate is positioned on four foam pieces of 10 mm and the ACTs are separated by a foam screen to prevent direct air-path transmission from the ACT to the PZT [12]. The ACT and the PZT are located at the same side of the plate. The position of the ACT and the PZT are drawn on the plate. At the ACT, a laser is attached, that will guide the transducer to the right position. The PZT is attached to the plate by shear gel ultrasonic couplant and adhesive tape.

Table 2 Gaussian pulse

Variable	350 kHz point focus	350 kHz plane wave	1 MHz plane wave
Sample frequency f_s [Hz]	$3.7 \cdot 10^7$ (f_c=233 kHz)	$4.1 \cdot 10^7$ (f_c=258 kHz)	$4.1 \cdot 10^7$ (f_c=738 kHz)
# samples	15079	15079	15000
ΔS [s]	$2E^{-8}$	$2E^{-8}$	$2E^{-8}$
# cycles	95	95	270
Time [s]	$3 \cdot 10^{-4}$	$3 \cdot 10^{-4}$	$3 \cdot 10^{-4}$

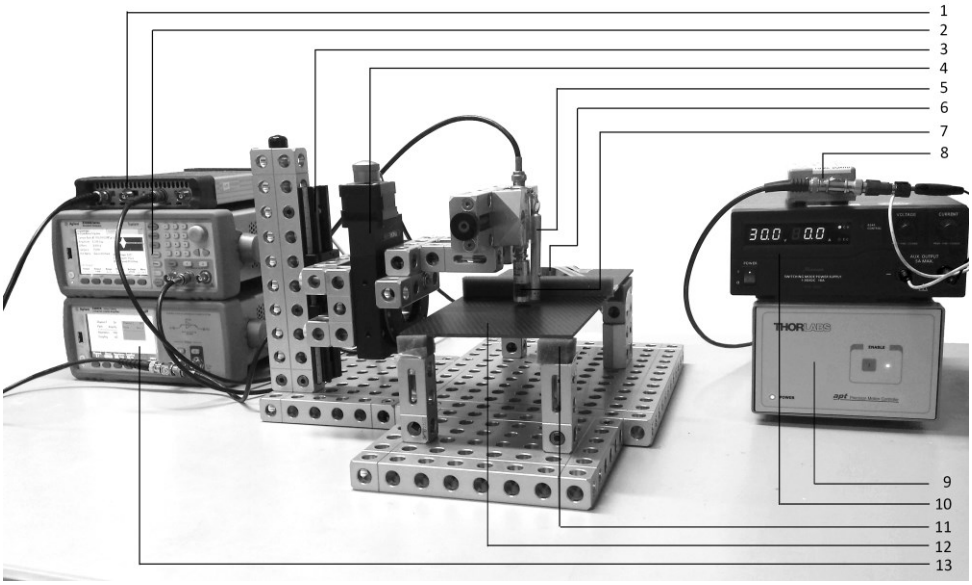

Figure 6. Experimental set-up

1	Oscilloscope (Picoscope 6402A)	8	Mistras amplifier 20/40/60 dB
2	Signal generator (Agilent 33522B)	9	Thorlabs apt precision motion controller BSC201
3	Vertical translation stage	10	Manson switching mode power supply
4	Thorlabs motorized 360° rotation stage NR360S	11	Foam
5	Laser	12	Carbon plate
6	Piezo electric transducer (Mistras WSα)	13	Pre-amplifier (Agilent 33502A)
7	Air-coupled transducer, see table 1		

Because of the large impedance mismatch that occurs between air and the CFRP plate [10], a large percentage of energy will be reflected at the boundaries, which results in a decreased signal to noise ratio (SNR). Therefore, the output signal is averaged to increase the voltage resolution and decrease the noise of the signal, assuming the noise is random [14]. Successive sample averaging of 11 bits and successive capture averaging of 10 waveforms are used to decrease the noise level. The number of samples for the DOE and damage test are calculated with the standard deviation and average of a pre-test. To achieve a confidence level of 95% and a maximum error of 1% of mean, the sample size is 110.

For damage detection, the signal is divided into four time windows (TWs) [2]. When the S_0 mode is generated (fig. 7), TW1 indicates the first reflection of the S_0 mode, TW2 is the first reflection of the A_0 mode and second reflection of the S_0 mode are shown respectively. TW3 indicates the rest of the reflections and TW4 contains the complete signal. When the A_0 mode is generated (fig. 8), the S_0 mode is damped out, which means that TW1 indicates the first reflection of the A_0 mode and TW2 shows the second and third reflection of the A_0 mode. Unfortunately, the signal has damped out before the third reflection is generated.

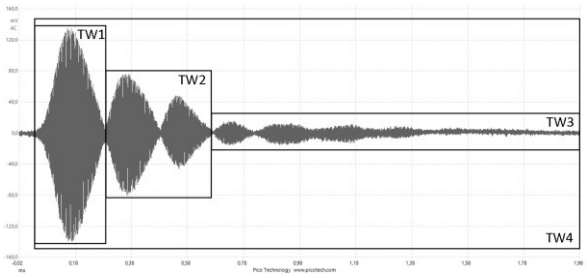

Figure 7. Time windows S_0

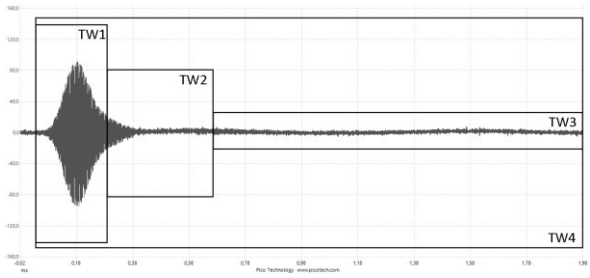

Figure 8. Time windows A_0

4. RESULTS AND DISCUSSION

4.1 Angle of incidence range

To create insight into the influence of different angles of incidence on the energy of the pulse and to reduce the amount of variables for the DOE, a pilot test with different angles of incidence was performed. The angle of incidence depends on the wave mode selected (S_0 or A_0), but can be set to an infinite number of angles as well ideally. The angle of incidence should be selected just before the critical angle [8]. To verify if this angle gives the best result, an experiment was performed with 41 different angles of incidence varying from -5° to 15° in steps of 0.5° for all three transducers. Results show the energy of the output signal in μJ for TW1 (first arrival) and TW3 (rest of the signal) for 41 different angles (fig. 9 – fig. 11).

The graphs are compared with the critical angles per transducer. The critical angles for the 350 kHz transducers for the S_0 and A_0 mode are respectively 3.12° and 7.37° and for the 1 MHz transducer 3.14° and 5.64° [8]. The peak energies of fig. 9 confirms the literature but the peak energies of fig. 10 and 11 are not before the critical angle and are therefore do not confirm the literature. Also the SNR is less for fig. 10 and 11 compared to fig. 9. The three angles at the peak energies for every transducer and for both wave modes are selected for the following test. The S_0 energy peaks are 1.5° to 2° before the calculated critical angle for the plane wave transducers and 1.5° after the critical angle for the point focus transducer. The peak energy is sensitive to the parameters of the time window, so the same time window is used as selected in the angle of incidence test.

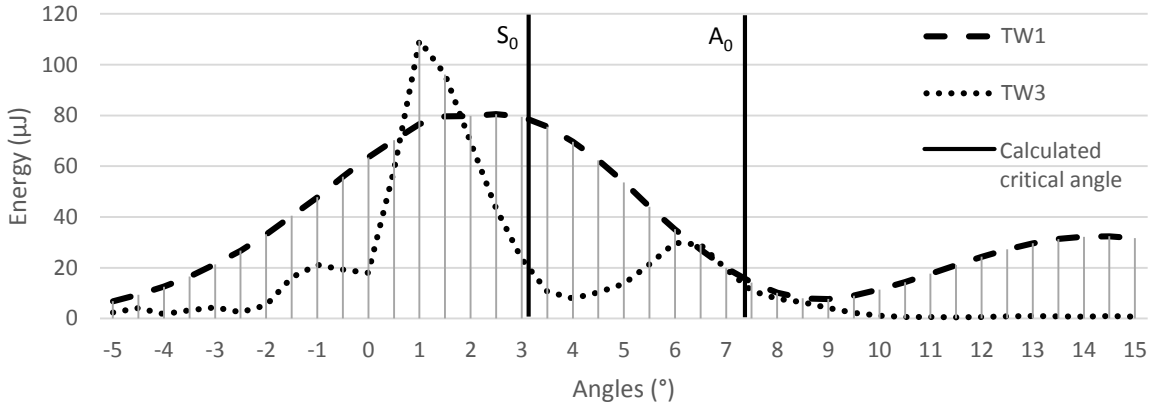

Figure 9. Angle of incidence 350 kHz plane wave transducer

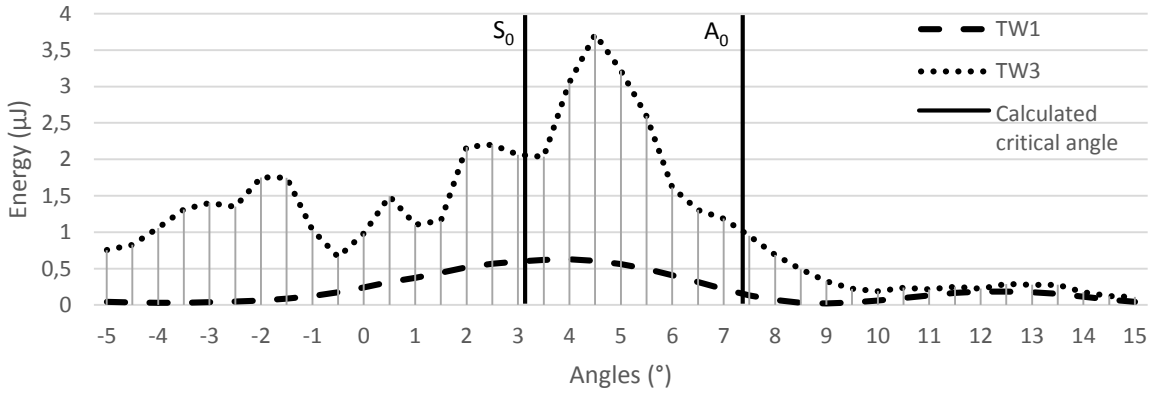

Figure 10. Angle of incidence 350 kHz point focus transducer

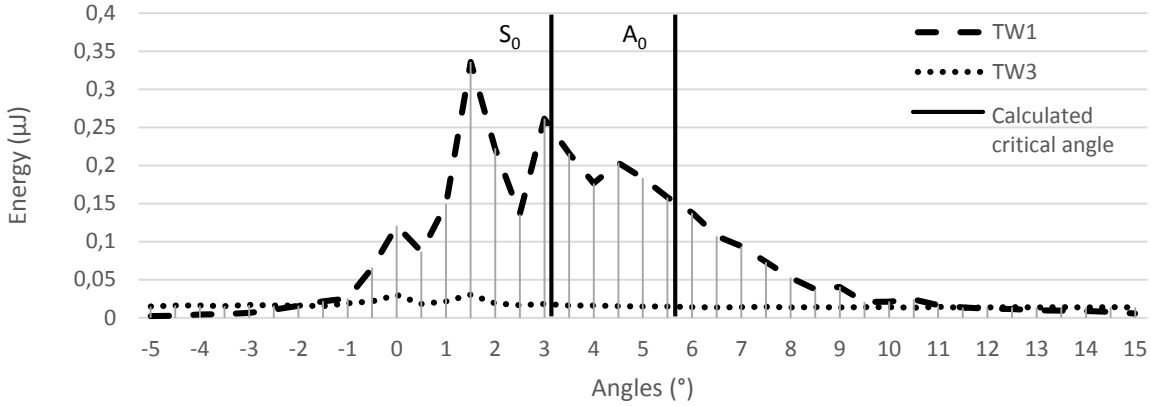

Figure 11. Angle of incidence 1 MHz plane wave transducer

4.2 Optimum setting variables

With the variable frequencies (350 kHz & 1 MHz), type of transducer (plane wave & point focus), distance between the transducer and the plate (less than the near field distance, between the near field distance and the focal length & more than the focal length), wave mode (S_0 & A_0) and angle of incidence (three angles at peak energies), the DOE is performed. The setting with the highest energy of the entire signal with a confidence level of 95% is the 350 kHz plane wave transducer at a distance less than the near field distance (33 mm), the S_0 mode applied at an angle of incidence of 2°. Comparing the individual settings, the 350 kHz plane wave transducer at a distance less than the near field distance for the S_0 mode and with an angle of incidence at the peak energy have the highest energy.

4.3 Damage detection test

To test if damage can be detected, a test is performed on a damaged plate with a hole of 10 mm at the center of the plate with four different settings (table 3).

Table 3 Settings damage detection test

Setting	Transducer	Distance transducer – plate	Wave mode	Angle of incidence
1	350 kHz plane wave	33 mm	S_0	2°
2	350 kHz plane wave	37 mm	A_0	14.5°
3	1 MHz plane wave	3 mm	S_0	1°
4	350 kHz point focus	33 mm	S_0	3°

To compare an undamaged signal with a damaged signal, first two reference measurements are performed with all four settings on an undamaged plate. After that, damage is applied on the same plate and two new measurements are performed. During all tests and while applying damage, the PZT is not removed. This means that no differences can occur in the signal related to the PZT. The four measurements are compared

by using fidelity and energy of the signal to determine which method has the best damage detection capability. This is defined as the largest difference between the undamaged and damaged signal, the number of time windows in which damage can be detected and the variances between the measurements.

The results are, that damage can be detected with the fidelity and energy method with all four settings (table 4). With the fidelity method, damage can be detected in TW3 and TW4, the average drop between undamaged and damaged is 12% and the variance between the measurements is $1.16 \cdot 10^{-2}$. For the energy method, damage can be detected in all four time windows, the average drop between undamaged and damaged is 66% and the variance between the measurements is $4.28 \cdot 10^{-16}$.

Table 4 Results damage detection test

Method	Time windows	Average drop Undamaged / damaged	Variances
Fidelity	TW3, TW4	12%	$1.16 \cdot 10^{-2}$
Energy	TW1, TW2, TW3, TW4	66%	$4.28 \cdot 10^{-16}$

4.4 Energy loss over distance

To create an insight in the energy loss over an increasing distance between the ACT and PZT, a test is performed with the best setting of the DOE with an increasing distance from 20 mm to 200 mm, with an interval of 2 mm. According to literature, the energy loss is an inverse square root function over distance [7].

The energy of the pulse has been calculated for all four time windows (fig. 12). It is noticeable is that the when TW1 peaks, TW2 drops and vice versa. This can be caused by an interference effect whereby multiple reflections are combined to one peak. And when the transducer is moved, these reflections are combined in a different way. Plotting a trend line, it confirms the literature that the attenuation in CFRP is an inverse square root function with the distance. The line that indicates the theory is an example for the energy drop in TW4. Other lines can be drawn for TW1 to TW3.

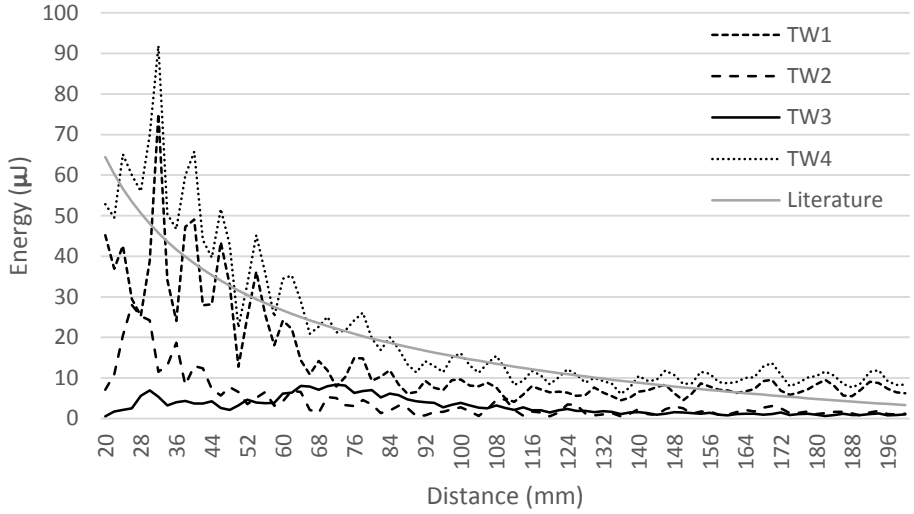

Figure 12. Distance between transducers

5. CONCLUSIONS

5.1 Design of experiments

For this part of the research, three different types of ACTs were available; 350 kHz plane wave, 350 kHz point focus and 1 MHz plane wave. Furthermore, the configuration can differ in wave mode (S_0 and A_0), angle of incidence and distance between the transducer and the plate. By performing a DOE, the best configuration is chosen by comparing the energies of the entire output pulse. With 95% confidence, the best configuration is the 350 kHz plane wave transducer, with a distance less than the near field distance (33 mm) between the transducer and the plate, the first symmetrical mode applied and an angle of incidence of 2°. Comparing the individual settings, the 350 kHz plane wave transducer, the first symmetrical mode, the angle of incidence at the peak energy and a distance between the transducer and the plate less than the near field distance are also indicated as best. By performing a test with an increasing distance between the ACT and the PZT is concluded that within the first 90 mm, the energy of the pulse fluctuates due to the interference effect. Plotting a trend line, the energy follows an inverse square root function, which means that after a while, the energy does not decrease rapidly. If damage can still be detected after 90 mm, large distances can be traveled in practical applications.

5.2 Damage test

USV is based on the principle that damage can be detected by comparing an undamaged signal with a damaged signal using fidelity. Four different settings are tested on an undamaged plate. After that, a hole of 10 mm is applied in the center of the plate and the four settings are tested again. Comparing both signals with fidelity can be concluded that damage can be detected with all four settings in TW3 and TW4. This means that ACTs can be used as alternative for PZTs in USV. Comparing the individual settings, the best settings to detect damages are the S_0 and A_0 mode of the 350 kHz plane wave transducer with a distance less than the near field distance (33 mm) and between the near field distance and the focal point (37 mm) and an angle of incidence of respectively 2° and 14.5°.

Because fidelity is not dependent on the amplitude (voltage) of the signal, and a voltage loss occurs when damage is present, another method for detecting damage has been performed. This method compares the energy of the output pulse of an undamaged plate with a damaged plate and expresses this in percentage of energy loss. With this method, damage can be detected in all four time windows, compared to two time windows for the fidelity method. Also, the difference in percentage between undamaged and damage is higher for the energy method compared to fidelity method. At last, the variances between the measurements is less for the energy method compared to the fidelity method. Based on these three results, damage can be detected best with the energy method.

ACKNOWLEDGEMENTS

The present work has been performed as a graduation research of G. Alleman at the University of Applied Sciences Amsterdam Aviation Studies, in cooperation with Delft University of Technology, supervised by M.M.J.M. Pelt and R.M. Groves. The authors would like to thank Ten Cate advanced composites for performing a tensile test on the composite material and Maria Barroso-Romero for calculating the dispersion curves.

REFERENCES

1. Diamanti, K., Hodgkinson, J. M. & Soutis, C., "Detection of low-velocity impact damage in composite plates using Lamb waves", *Structural Health Monitoring*, 2004, 3(1), 33-41.
2. Hopman, R. & Zaalberg, J.P., "Ultrasonic Verification", 2013, Hogeschool van Amsterdam. Unpublished.
3. Ambrozinski, L., Piwakowski, B., Stepinski, T., & Uhl, T., "Application of air-coupled ultrasonic transducers for damage assessment of composite panels", 2012, Proc. the 6th EWSHM.
4. de Carvalho, P. A. V. O., "Detection of multiple low-energy impact damage in composites plates using Lamb wave technique".
5. Kessler, S. S., Spearing, S. M. & Soutis, C., "Damage detection in composite materials using Lamb wave methods", *Smart Materials and Structures*, 2002, 11(2), 269.
6. Nagy, P. B., "Introduction to ultrasonics", University of Cincinnati, department of aerospace engineering & engineering mechanics, 2001.
7. Barroso-Romero, M., Barazanchy, D., Martinez, M., Groves, R.M. & Benedictus, R., "Time reversal of Lamb waves for damage detection in thermoplastic composites", *ICAST2013: 24th International Conference on Adaptive Structures and Technologies.*
8. NDT Education Resource Center, "The Collaboration for NDT Education", Iowa State University, 2001-2012. Retrieved February 11, 2014, from www.ndt-ed.org.
9. University of Dayton, "Wave Equations and Impedance: Transverse Waves in a String and sound", 2012, http://academic.udayton.edu/LenoPedrotti/text232/ch7.pdf
10. Castaings, M. & Cawley, P., "The generation, propagation, and detection of Lamb waves in plates using air-coupled ultrasonic transducers", *The Journal of the Acoustical Society of America*, 1996, 100(5), 3070-3077.
11. Olympus NDT, "Ultrasonic transducer technical note", 2006, Panametrics-NDT
12. Castaings, M. & Hosten, B., "Lamb and SH waves generated and detected by air-coupled ultrasonic transducers in composite material plates", *Ndt & E International*, 2001, 34(4), 249-258.
13. Duflo, H., Morvan, B. & Izbicki, J. L., "Interaction of Lamb waves on bonded composite plates with defects", *Composite structures*, 2007, 79(2), 229-233.
14. Bishop, C. & Kung, C., "Effects of Averaging to Reject Unwanted Signals in Digital Sampling Oscilloscopes", *Autotestcon*, 2010, IEEE (pp. 1-4).